

## Charging effects observed in $\text{YBa}_2\text{Cu}_3\text{O}_{7-x}$ films: Influence of oxygen ordering

N. Chandrasekhar, Oriol T. Valls, and A. M. Goldman

*Center for the Science and Application of Superconductivity and School of Physics and Astronomy, University of Minnesota, Minneapolis, Minnesota, 55455*

(Received 17 September 1993)

The chain oxygen dynamics of  $\text{YBa}_2\text{Cu}_3\text{O}_{7-x}$  have been investigated using a Monte Carlo simulation of the asymmetric next-nearest-neighbor Ising model for the oxygen atoms in the basal plane. The effect of an externally applied electric field is shown to change the basal plane coordination of Cu ions, resulting in a change in the carrier doping of the  $\text{CuO}_2$  planes. Good quantitative agreement is obtained with the asymmetry observed in field effect experiments. We present results under different applied external fields, study the long-term ordering dynamics and investigate the effect of oxygen content on the phenomenon. We discuss the relevance of our results to studies of point-contact spectroscopy, tunneling, electromigration, and the enhancement of superconductivity by photoexcitation. We also present a historical perspective in terms of the Verwey transition in  $\text{Fe}_3\text{O}_4$ , which involves a similar mechanism.

### I. INTRODUCTION

The effects of applied electric fields on the properties of superconducting thin films have been interpreted as arising from changes in the charge-carrier density in a film, without altering its chemical structure.<sup>1-3</sup> Considerable interest exists in three-terminal devices exploiting this phenomenon.<sup>4</sup> However, a substantial body of experimental evidence indicates that the high mobility of oxygen in  $\text{YBa}_2\text{Cu}_3\text{O}_{7-x}$  (YBCO) is an issue that cannot be ignored. In point-contact spectroscopy, relaxation effects attributable to oxygen motion have been observed by Rybal'chenko *et al.*<sup>5</sup> Investigations of oxygen-deficient  $\text{YBa}_2\text{Cu}_3\text{O}_{7-x}$  single crystals, in which increases of the transition temperature by as much as 30 K were observed by room-temperature aging,<sup>6,7</sup> demonstrate significant oxygen mobility. Electromigration studies have also demonstrated the importance of oxygen order in determining the normal state and superconducting properties of  $\text{YBa}_2\text{Cu}_3\text{O}_{7-x}$ .<sup>8</sup> High oxygen mobility leads to enhanced ordering in single crystals of this oxygen-doped compound, even at room temperature. The relevant parameter determining the doping of the  $\text{CuO}_2$  planes and hence the transition temperature at a fixed oxygen content is the nature and extent of oxygen in the basal plane.<sup>6,7</sup> An activation energy of  $0.97 \pm 0.03$  eV has been measured for oxygen by tracer diffusion.<sup>9</sup> Despite this apparently high activation energy, it has been demonstrated that significant oxygen rearrangement and ordering can occur from room temperature, down to 50 K.<sup>10</sup>

In earlier work,<sup>11</sup> using a modification of the asymmetric next-nearest-neighbor Ising (ASYNNNI) model, we demonstrated that considerable rearrangement of chain oxygen occurs upon the application of an external electric field, causing a change in the doping of the  $\text{CuO}_2$  planes in YBCO. As a result, the carrier concentration, which is related to the ordering of oxygen vacancies, is altered. Results were presented in Ref. 11 for a macroscopic field of  $0.1 \text{ V/\AA}$  and an oxygen content of 6.75 ( $x = 0.25$ ), where the ratio of the change in resistance at

positive bias to that at negative was compared to the ratio of the change in doping evaluated from the model, and good quantitative agreement was obtained. Further, the time constants observed experimentally and those predicted by the model were also found to be in good agreement. In the present work, we investigate the long-term dynamics (i.e., study the phenomenon until steady state is achieved at a fixed bias), and study the effects of changes in the applied field, of changes in the dielectric constant of the material (relevant in determining the local field through the Lorentz relation) and of variations of the oxygen content. The implications of the electric-field-induced ordering of oxygen for studies of point-contact spectroscopy,<sup>5</sup> electromigration<sup>8</sup> and the enhancement of superconductivity by photoexcitation<sup>10,12</sup> will also be discussed. Finally, we present a historical perspective in terms of the Verwey transition in  $\text{Fe}_3\text{O}_4$ , which appears to have a similar physical origin.

### II. MODEL AND METHODS

The starting point for the study of the relation between oxygen ordering and hole concentration in YBCO in the presence of an external electric field is the standard description of oxygen ordering in the basal plane in terms of the ASYNNNI model. This model was first proposed in Ref. 13, and has been successful in explaining the zero-field phase diagram of YBCO. One introduces an Ising variable  $\sigma_i$ , at each oxygen site ( $i$  is the site index). This variable takes the value  $+1$  if the site is occupied by an oxygen atom, and  $-1$  if it is empty (occupied by a vacancy). The ASYNNNI Hamiltonian is then written as

$$H_0 = V_1 \sum_{ij}^{\text{NN}} \sigma_i \sigma_j + V_2 \sum_{ij}^{\text{NN(Cu)}} \sigma_i \sigma_j + V_3 \sum_{ij}^{\text{NNN}} \sigma_i \sigma_j. \quad (1)$$

the sites  $i, j$  are all the oxygen sites in the basal plane, and the symbols NN and NNN mean that the sum over  $i$  and  $j$  extends over "nearest neighbors" and "next nearest neighbors," respectively. The basal plane is schematized in Fig. 1 where the interactions  $V_1$ ,  $V_2$ , and  $V_3$  are indi-

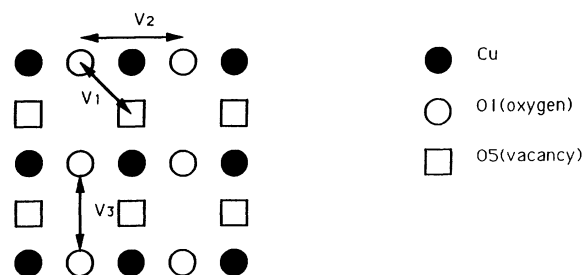


FIG. 1. Basal plane of YBCO. Filled circles are Cu. The interactions in Eq. (1) are indicated.

ated. The ground state of this Hamiltonian was determined in Ref. 14 as a function of the ratios  $V_2/V_1$  and  $V_3/V_1$  ( $V_1 > 0$ ). These results were later rederived analytically.<sup>15</sup> Since the interaction  $V_2$  is mediated by an intervening Cu ion, it has to be attractive, while  $V_1$  and  $V_3$  are positive and  $V_3 < V_1$ . For YBCO, the values of these parameters have been calculated by Sterene and Wille<sup>16</sup> as being 0.094,  $-0.032$ , and  $0.015$  eV, respectively. These are the values we shall use throughout this paper.

To include the electric-field effects, we add a term to the Hamiltonian to take into account the interaction of the external field with the oxygen electric dipole moments. It is an experimentally well-established but not generally appreciated fact that the thermodynamic average of these dipole moments is nonzero in YBCO and similar compounds. There is a very large body of experimental evidence<sup>17–23</sup> showing the existence of permanent electric dipole moments in these materials. We do not consider dipole moments associated with species other than oxygen atoms in the basal plane. The reason for this is that the basal plane oxygen is the only relevant species in determining the hole concentration in the  $\text{CuO}_2$  planes, which is the origin of the physical phenomena discussed in this paper. Significant evidence exists for the presence of deep double well potentials in YBCO.<sup>17–23</sup> This confirms that the dipole configurations are indeed permanent, with the coercive fields being very large in comparison to the electric fields considered in this work. Of course, the coexistence of local electric dipole moments and superconductivity is not peculiar to high- $T_c$  superconductors, it occurs in “classical” superconductors such as doped  $\text{SrTiO}_3$ . Thus, these moments must be included in a discussion of electric-field effects. We do this by adding the appropriate interaction term to Eq. (1). Our Hamiltonian is, therefore,

$$H = H_0 - \epsilon \cdot \sum_i \frac{1}{2} (1 + \sigma_i) \mathbf{p}_i, \quad (2)$$

where  $\epsilon$  is the local electric field and  $\mathbf{p}_i$  the electric dipole moment of an oxygen at site  $i$ . The combination  $\frac{1}{2}(1 + \sigma_i)$  is a Kronecker delta which vanishes when the  $i$ th site is unoccupied. The value of  $\mathbf{p}_i$  is site specific: the electric dipole moment of the oxygen atom depends on its electronic environment. Values of  $\mathbf{p}_i$  have been calculated using a shell model.<sup>24,25</sup> These values depend on the

oxygen content. At  $x = 0.25$ , for example, one has  $p_i = 0.003$  eÅ for O1 sites, and  $0.013$  eÅ at O5 sites. These sites are labeled in Fig. 1. The variation of the dipole moment with oxygen content in YBCO is shown in Fig. 2. We are concerned only with the magnitude of the dipole moment as it turns out that its largest component is by far that along the  $c$  crystallographic direction at an oxygen content of 6.75. The magnitude of this component decreases with decreasing oxygen content. While the other components along the  $a$  and  $b$  crystallographic axes increase in magnitude with decreasing oxygen content.

A deviation from linearity in the thermal expansion is an indication of the existence of spontaneous polarization.<sup>26</sup> Such a phenomenon has been observed in bar-shaped specimens of  $\text{GdBa}_2\text{Cu}_3\text{O}_{7-x}$ .<sup>19</sup> The spontaneous polarization has been evaluated from the strain data and is consistent with atomic displacements of  $0.05$ – $0.1$  Å.<sup>19</sup> We stress the fact that the dipole moments (Fig. 2) we use for the basal plane oxygen are consistent with these values of atomic displacements reported in the literature.

Let us now consider the energetics associated with Eq. (2). Typical potential differences used in field effect experiments are in the range  $3$ – $10$  V for films of thicknesses between  $12$  and  $100$  Å.<sup>2,3</sup> In YBCO these thicknesses are smaller than the Debye screening length, so that the electric field penetrates the sample. The weak screening is the result of YBCO being a very poor conductor in the normal phase. The carrier concentration in well-oxygenated YBCO is at least 2 to 3 orders of magnitude lower than that of a metal and we expect the screening length to be larger by a factor of  $10$ – $30$ . YBCO surfaces are known to be very reactive and this causes further reduction in the oxygen content and carrier concentration in very thin films, such as those used in field-effect studies. We consider the field associated with a potential drop of  $10$  V over a  $100$ -Å-thick film, a fairly conservative estimate of the macroscopic field. One can then estimate the local field [the quantity  $\epsilon$  in Eq. (2)] through the use of the Lorentz relation. To do this, we use the static dielectric constant value of  $\sim 400$  given by Testardi *et al.*<sup>27</sup> The resulting local field is, therefore, enhanced by a factor of about  $100$  with respect to the macroscopic field. For lower dielectric constants the local field would be enhanced by a correspondingly smaller factor. Typical

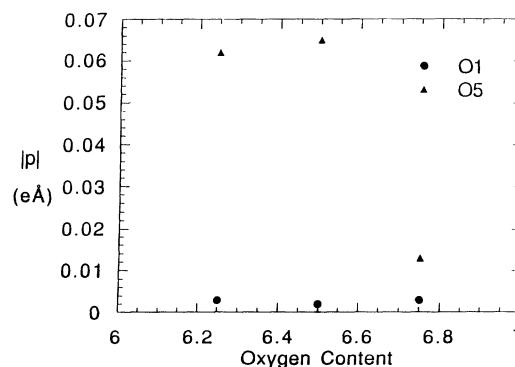
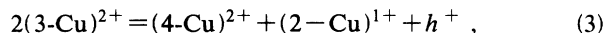


FIG. 2. Dipole moment  $|p|$  in units of eÅ of the basal plane oxygen as a function of oxygen content, as calculated in Ref. 25.

configurational energies per oxygen site at zero field, as calculated from Eq. (1) are about 0.4 eV. It follows from the above arguments that the additional energy added to Eq. (2) by the field term is about 0.16 eV at a dielectric constant of 400 and a macroscopic field of 0.1 V/Å, and therefore makes a nontrivial contribution to the configurational site energy. On the other hand, the strain energy associated with the 2.2% misfit of lattices of the YBCO film and the SrTiO<sub>3</sub> substrate has been ignored in these calculations. Although it is not at all clear how the interaction energies  $V_i$  change as a function of strain, it is, however, possible to evaluate the strain energy in the film, using elastic constants published in the literature,<sup>24</sup> and thus determine a strain energy per oxygen atom in the basal plane. This contribution turns out to be of the order of 0.02–0.04 eV, which can clearly be ignored in comparison to the electric-field-induced energy.

Qualitatively, when an electric field is turned on, the oxygen atoms will migrate so as to minimize their energy associated with Eq. (2). The response to a field which influences oxygen ordering is a consequence of the fact that the dipole moments on the O1 and O5 sites are different. Oxygen atoms will then diffuse from the O1 to the O5 sites if a field were applied along the direction of the permanent dipole moments and vice versa. This diffusion in response to the field will be opposed by the remaining terms in the Hamiltonian so that a new equilibrium will be reached. An important consequence of this process will be a change in the number of carriers (holes) as discussed by Wille and de Fontaine and various co-workers.<sup>13,14,16</sup> The Cu ions in each basal plane are two-, three-, or fourfold coordinated with oxygen. Since the apical O4 sites are always occupied, these coordinations correspond to chain segment configurations  $V$ -Cu- $V$ ,  $V$ -Cu-O, and O-Cu-O, respectively ( $V$  stands for a vacancy), as one can see in Fig. 3. As the Cu coordination changes, the number of holes increases or decreases. Threefold coordinated Cu ions are in a 2<sup>+</sup> oxidation state and a configuration of higher energy, as are fourfold coordinated Cu ions, but the twofold coordinated ions are in a 1<sup>+</sup> oxidation state. Thus one can write the reaction



where  $h^+$  denotes a hole. The forward reaction adds holes and increases the doping of the CuO<sub>2</sub> planes

whereas the reverse reaction reduces the number of holes and reduces the doping of the CuO<sub>2</sub> planes. We see then how the electric field can induce a change in the number of carriers by changing the coordinations of the basal plane Cu in a process not involving charge transfer. A similar mechanism was used to explain the increase in the transition temperature of quench-reduced oxygen content single crystals upon room-temperature aging.<sup>6,7</sup> In these aging experiments, however, the forward reaction dominates and it is impossible to achieve the reverse reaction unless a high enough temperature is reached. The above field-effect mechanism is clearly distinct from the classical metal field effect or piezoelectric effects.

We now explain the procedure to implement the calculations. The basic idea is to perform a Monte Carlo study taking Eq. (2) to be the Hamiltonian. As explained above and in Ref. 11, there are no free parameters in Eq. (2): all quantities are taken from previous independent calculations and experiments. The simulation uses the standard Metropolis algorithm to follow the evolution of the Cu coordinations in the basal plane in the presence of a field. The simulations are quite easy and not at all technically demanding from a computational point of view. We use a lattice of  $N^2$  sites, where  $N$  equals 64 and we have verified that the results are free of finite-size effects in the time scales considered. It is necessary to estimate the relation between Monte Carlo time, given in Monte Carlo steps per site (MCS) and physical time. Ceder and co-workers<sup>7,28</sup> studied oxygen diffusion in the  $a$ - $b$  plane and concluded, by comparing the results of their simulations with known oxygen diffusion constants<sup>9</sup> that 1 MCS is approximately equal to 1 min at room temperature. We stress that this assignment holds only in order of magnitude. Since it is merely a determination of an attempt rate only weakly temperature dependent and the effects of field and temperature are in the opposite direction, we can take the above assignments as an appropriate order of magnitude estimate in comparing our time scales with experimental results.

We begin by randomly distributing the oxygen atoms (at a fixed value of  $x$ ) among the two kinds of sites and attain the equilibrium distribution between them, by using Eq. (1) for approximately 1000 MCS. We then start our Monte Carlo simulation of the effects of an externally applied electric field, using the full Hamiltonian (2) at the desired value of the applied field. We use a temperature of 100 K in order to facilitate comparison with experi-

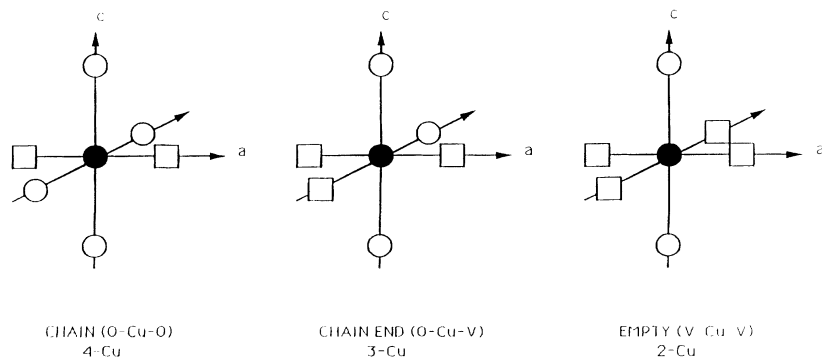


FIG. 3. Possible coordinations of basal plane Cu. Open circles are oxygen atoms and the vacancies are denoted by unfilled squares.

mental measurements. We monitor the number of oxygens at each kind of site, and track the basal plane Cu coordinations for up to several hundred MCS per site, at which point these numbers have stabilized. We are interested in relatively short-time behavior and in a classical field-effect device, the temporal response of the device is governed by the  $RC$  time constant (usually of the order of microseconds), which is extremely short compared to the time scales we consider. From the time evolution of the changes in the coordination of the basal plane Cu atoms it is an easy matter to determine the change in the number of holes by using Eq. (3).

### III. RESULTS

We present our results in Figs. 4–8. These cover two values of the oxygen substoichiometry  $x$  ( $x = 0.25$  and  $0.5$ ) and two values of the applied field,  $0.1$  and  $0.2 \text{ V/\AA}$ . The values of  $x$  correspond to concentrations over the usual range in experimental work and for which results are available. The applied fields are also in the appropriate experimental range. All figures show the same general trends: in a field antiparallel to the permanent dipoles the twofold and fourfold coordinated Cu fractions decrease, while the threefold coordinated Cu fraction increases. This causes a reduction in the doping of the  $\text{CuO}_2$  planes according to Eq. (3), where the reverse reaction is the one that is taking place. This direction of the field corresponds to that of “positive bias” in the experiments.<sup>2,3,29</sup> The opposite effect is observed for a field along the permanent dipoles (negative bias). Now the forward reaction in Eq. (3) dominates and increases the doping of the  $\text{CuO}_2$  planes. Cu environments with more than two basal plane oxygen atoms are seldom observed as they are strongly suppressed by the highly repulsive  $V_1$  interaction between nearest neighbors. Most of the changes take place relatively quickly (i.e., in the first hundred or so MCS), as can be seen in Fig. 4, where we plot the changes in the fraction of Cu atoms in a particular coordination geometry as a function of MCS per site.

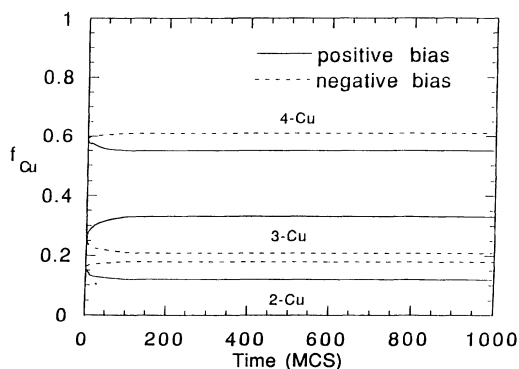


FIG. 4. Fraction  $f$  of Cu atoms in a given coordination geometry as a function of simulation time in units of Monte Carlo Steps (MCS), at positive and negative biases. Note the asymmetry of the results. The parameters used are  $x = 0.25$ , applied field of  $0.1 \text{ V/\AA}$ , and a dielectric constant of 400 (see text).

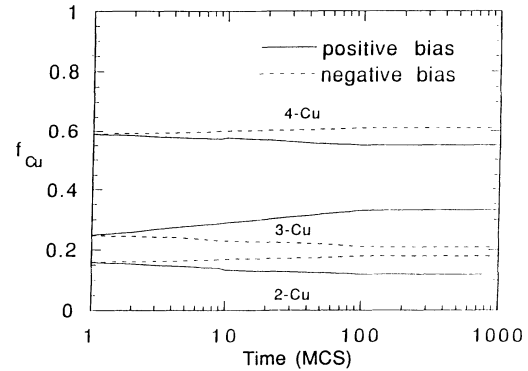


FIG. 5. The results of Fig. 4 with  $f$  plotted on a logarithmic scale.

After the first hundred MCS, no change in the fraction of Cu atoms in a particular coordination is seen in the log plot shown in Fig. 5. Both Figs. 4 and 5 are for an applied field of  $0.1 \text{ V/\AA}$ , a static dielectric constant of 400, and an oxygen content of 6.75 per formula unit. The asymmetry of the effect is clearly visible, in the sense that the change in the fraction of the threefold coordinated Cu atoms is not the same at identical values of positive and negative bias. Such an asymmetry has been observed experimentally in field-effect studies.<sup>2,3,29</sup> If classical charge transfer were the only operative mechanism for the experimental observations, one would be hard pressed to explain the origin of this asymmetry. In order to eliminate unknown parameters in comparing the model with experiment, we study the ratio of changes in the resistance at 100 K which follow from a change in the sign of the bias voltage. The ratio of the magnitudes of the change in resistance at this field in the experiment is 1.75.<sup>3,29</sup> Our results from the model (Figs. 4 and 5) yield a value of 2, in good agreement with the observations. This agreement is very satisfactory when one realizes that there are no adjustable parameters in our theory, and that the Monte Carlo probabilities depend exponentially upon the values of the parameters considered.

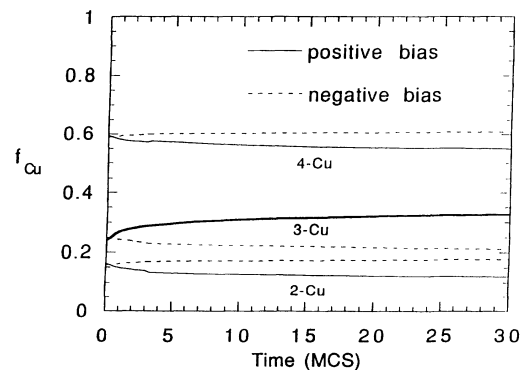


FIG. 6. Effect on fraction  $f$  of Cu atoms in a given coordination geometry of increased field. Parameters used are  $x = 0.25$ , an applied field  $0.2 \text{ V/\AA}$ , and a dielectric constant of 200. The time is in units of MCS.

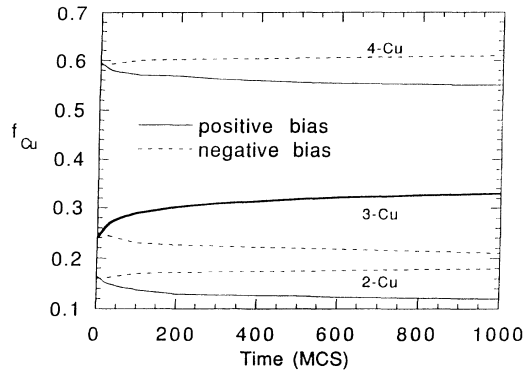


FIG. 7. Effect on the fraction  $f$  of Cu atoms in a given coordination geometry of a reduced dielectric constant. The field and  $x$  are as in Figs. 4 and 5, but the dielectric constant is 100.

In the remaining figures, we show the evolution of the fractional CU coordinations only on a linear scale, until equilibrium is attained. The dependence of the results on the magnitude of the field can clearly be seen to be weak in comparison to the dependence on oxygen content. Increasing the magnitude of the field changes the activation energy for oxygen motion. Clearly, there are limitations on the values of parameters that can be chosen in our model, in the sense that the product of the dipole moment and the local field should not approach the site energy determined from the ASYNNNI Hamiltonian. There is some uncertainty as to the value of the dielectric constant of the YBCO films used in field-effect experiments. For this reason, we consider effects of the variation of the dielectric constant. We present results for three other cases, viz,  $x=0.25$  with a field of  $0.2 \text{ V/\AA}$  and a dielectric constant of 200,  $x=0.25$  with a field of  $0.1 \text{ V/\AA}$  and a dielectric constant of 100, and  $x=0.5$  with a field of  $0.1 \text{ V/\AA}$  and a dielectric constant of 100. The results for the first case are shown in Fig. 6. The asymmetry is unchanged, but equilibrium is attained in a shorter time interval since the field has been enhanced. In Fig. 7, we show the results for the second case, where

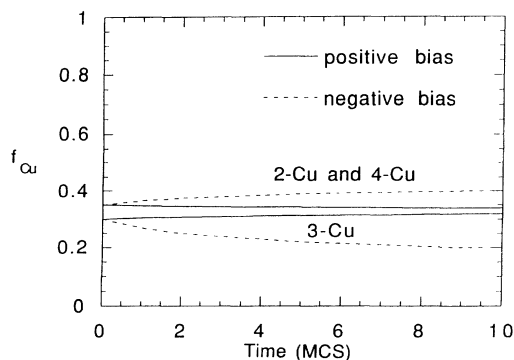


FIG. 8. The field effect at reduced oxygen content. All parameters are as in Fig. 7, except now  $x=0.5$ . Note the changed asymmetry (relative to Fig. 7) and the faster temporal response.

it clearly takes a longer time to attain equilibrium, since the dielectric constant is small, and the electric dipole contribution to the activation energy is correspondingly lower.

The dependence on  $x$  is somewhat more pronounced, although there are no changes in qualitative behavior. As one would expect, an increase in the number of vacancies, which accompanies an increase in  $x$ , and also the corresponding increase in dipole moment caused by an increase in the asymmetry of the electronic environment in which the atoms reside (Fig. 2), imply an increase in the field effect. In Fig. 8 we show our results for the last case, i.e., an oxygen content of 6.5, a field of  $0.1 \text{ V/\AA}$ , and a dielectric constant of 100. The asymmetry has changed fairly dramatically. A very small change is seen at positive bias and a very large one at negative bias. The ratio of changes in the doping at positive and negative biases is now less than 1; i.e., 0.2 to be precise. Thus, by merely changing the oxygen content, the asymmetry of the effect has been changed by an order of magnitude. This occurs because at these lower oxygen contents, the oxygen chains in the basal plane are already so fragmented that further fragmentation, favored by positive bias field, is strongly suppressed, while chain healing favored by negative bias is enhanced. These results are consistent with experimental observations of Xi *et al.*,<sup>3</sup> who found that in order to attain identical magnitude of changes in resistance at positive and negative bias, for a  $50\text{-\AA}$ -thick YBCO film (which has a transition temperature of about 13 K in zero applied field and hence an oxygen content that is probably closer to 6.5) the gate voltage at positive bias had to be about 10 times that at negative bias. In light of the sensitivity of the asymmetry of the effect to oxygen content, it appears that at some intermediate oxygen content between 6.5 and 6.75, the asymmetry vanishes. We do not know of any straightforward technique to determine this value. The results demonstrate another important point about oxygen ordering: it takes more energy to break chains in the basal plane than to form them. This follows directly from the work of de Fontaine *et al.*,<sup>30</sup> in which it is pointed out that "oxygen atoms in the basal plane of YBCO, at equilibrium, will always form the longest possible chains if given enough time to migrate, thereby minimizing the number of energetically unfavorable chain-end configurations." One should note that with decreasing oxygen content, there will eventually be a transformation from an orthorhombic to a tetragonal structure. At this point the O1 and O5 sites will be similar and the model used here will no longer bring about an electric-field driven effect.

In summary, at a negative bias the number of holes available to the  $\text{CuO}_2$  planes increases. One has a reduction in the number of chain fragments (healing), which increases the doping by minimizing the fraction of energetically unfavorable 3-Cu chain ends. For the opposite bias, one has chain fragmentation and a decrease in the number of holes. This follows from the results shown, together with Eq. (3). At larger values of  $x$ , we find that the asymmetry increases, which is again consistent with experimental results.<sup>3</sup>

Our simulations have considered only nearest-neighbor

hopping. We now discuss the possible relevance of next-nearest-neighbor jumps in the basal plane, since recent experimental evidence suggest that these probably occur to a nontrivial extent.<sup>31</sup> The attempt frequency for oxygen for nearest-neighbor hopping may be readily evaluated from experimental measurements of the diffusion constant  $D_0$ .<sup>9</sup> This turns out to be of the order of  $10^{12}$  attempts per second. Since it is difficult to deconvolute the contributions of nearest-neighbor and next-nearest-neighbor hopping to the diffusion constant, at the present time it is difficult to assign an attempt frequency for next-nearest-neighbor jumps with any degree of certitude. The Monte Carlo code may, however, be easily modified to take into account such hopping. Inclusion of these jumps might change the shape of the curves in Figs. 4–8, but would not modify the final equilibrium values attained.

#### IV. DISCUSSION

The phenomenon of oxygen-ordering-induced hole doping is clearly an important one and is of relevance not merely for the field-effect studies, but also for studies of point-contact spectroscopy, electromigration, and enhanced and persistent photoconductivity, as pointed out in the Introduction. One can readily evaluate the change in the doping that can be achieved at a certain field, using Eq. (3). This turns out to be of the order of  $10^{13}/\text{cm}^2$ . Xi *et al.*<sup>3</sup> estimate the changes in carrier concentration in their experiments to be of the order of  $10^{14}/\text{cm}^2$  using  $(\Delta R/R) = -(\Delta N/N)$ , where  $R$  is the measured resistance and  $N$  is the carrier concentration. This agreement is indeed very satisfactory, when one considers the nature of Monte Carlo simulation, where results can depend strongly upon the parameter values chosen and the fact that we have not used a single free parameter.

We now consider the characteristic times. The temporal response of a field-effect device has been studied both by Xi *et al.*<sup>3</sup> and by Mannhart.<sup>29</sup> Relaxation effects, which can be fitted to a time constant of the order of minutes, are observed.<sup>29</sup> Further, in both experiments, the temporal response is not at all consistent with an interpretation based on charge transfer by the field effect. This is because the response of a field-effect device is determined by the  $RC$  time constant.<sup>32</sup> The  $RC$  time constants for both sets of experiments are in the microsecond range, while the experimentally observed response is clearly much slower. Further, the response is fairly sensitive to the oxygen content, applied field, and dielectric constant, in agreement with the present considerations.

Many studies of tunneling spectra are in the point-contact mode or use a scanning tunneling microscope in a soft point-contact mode. Although it is quite difficult to estimate the electric-field distribution around the region of contact or the tunneling tip, at the biases ( $-0.1$ – $0.1$  V) used in such studies, we estimate that the fields seen by the oxygen atoms are comparable to the values considered here assuming the field to be screened within the Debye length in the normal state. At the superconducting transition, the dielectric constant diverges, theoretically

making the field seen by the oxygens infinite. These effects can cause significant rearrangement of oxygen atoms, thereby changing the intrinsic nature of the normal metal or the superconductor. Since the surfaces of these compounds form a natural barrier by oxygen depletion, which reduces the carrier concentration, the nature of the barrier may also be changed to a nonideal one by the external field. Asymmetry in the conductance (at positive and negative bias) is seen both in the normal state and in the gap feature in the superconducting state. This asymmetry is found to depend sensitively upon the oxygen content of the material. Further, temporal variations in tunneling spectra, on a time scale inconsistent with quasiparticle lifetimes or relaxation rates have been observed by van Bentum *et al.*<sup>33</sup> Electromigration studies<sup>8</sup> are explicable when one acknowledges the presence of permanent dipole moments on the basal plane oxygen. Depending on the geometry of the bias with respect to the polarization, it is favorable for the oxygen to either order or disorder and the results are sensitive to the field rather than, as previously thought, the current.<sup>34</sup> In field ion microscopy studies, application of a negative bias has been found to change the nature of the surface from insulating to metallic. The magnitude of the fields applied are comparable to those considered in this work and the experimental observations are consistent with our ideas.<sup>35</sup>

As mentioned earlier, the oxygen in the basal plane always tends to order in a manner that maximizes the chain lengths. This is particularly true at zero bias. Thus, it is not surprising that the conductivity of crystals and films can be enhanced significantly by irradiating them with light with a photon energy of 1.9 eV. The activation energy for a nearest-neighbor jump, in the absence of a vacant nearest-neighbor site, is of the order of 1.6 eV. We caution that this is a number that sensitively depends on the oxygen content and assumes a vacancy diffusion mechanism.

The transport of electrons in polar crystals has been investigated by Feynman and co-workers.<sup>36–38</sup> The electron interacts with the surroundings in the polar crystal, the effect of the interaction being to surround the electron with a distorted lattice: a cloud of optical phonons. Significant corrections (changes of an order of magnitude or larger) can occur to the effective mass, since it scales as the square of the coupling constant. Such large changes can be expected to have effects on transport properties as well as tunneling spectra.<sup>39</sup>

In this work, we have neglected elastic distortion effects caused by strain (due to lattice misfit between the film and the substrate), the effects of twins, grain boundaries, and other microstructural features, and also surface effects such as image charges and trapping sites. It is not clear at the present time whether there exists a formalism which can incorporate such effects into a model of the type presented here. Such terms will lead to corrections, but we expect them to be fairly small in comparison with the charge transferred by oxygen motion. The motion of oxygen can also lead to noise, and Liu *et al.*<sup>40</sup> report  $1/f$  normal-state resistance fluctuations at room temperature which they attribute to oxygen motion. A minimum in the noise is seen at an oxygen

content of 6.5. At this oxygen content the OII ordering is observed in the basal plane, a configuration which has the lowest free energy and is most stable. Naturally, the activation energy for oxygen motion is highest for this configuration, and consequently a reduction in noise is expected. It is also worth noting that YBCO exhibits a  $1/f$  noise magnitude significantly higher than other cuprate superconductors, which do not possess a chain structure.

The mechanism of the oxygen order-disorder transition in the basal plane of YBCO, induced by an external field, closely parallels that of the Verwey transition in  $\text{Fe}_3\text{O}_4$ .<sup>41</sup> An anomaly in the temperature dependence of the electrical conductivity is seen in  $\text{Fe}_3\text{O}_4$ . Around 120 K, the conductivity decreases by about two orders of magnitude. In this transition the driving force is provided by the Coulomb interaction between the  $\text{Fe}^{2+}$  and  $\text{Fe}^{3+}$  sites and temperature. The energy of the lattice is lowered when the ions distribute themselves so as to make the  $\text{Fe}^{2+}$  and  $\text{Fe}^{3+}$  pairs nearer and pairs of Fe with the same valence farther away. The state with the lowest energy is not realized except at 0 K. At finite temperatures, the state of lowest free energy is realized. Verwey applied the theory of order-disorder transitions to this system in order to explain the anomalous behavior of the resistivity in  $\text{Fe}_3\text{O}_4$ . Clearly, moving the ions in a lattice changes the electronic structure and hence the doping.

## V. CONCLUSIONS

In conclusion we have used a modified ASYNNNI model to study the effect of an external electric field on oxygen ordering in YBCO. We find that a significant amount of basal plane oxygen rearrangement takes place which changes the doping of the  $\text{CuO}_2$  planes. The magnitude of the effect and its temporal response depend upon the oxygen content, the applied field and the dielectric constant of the material. The phenomenon is important not only in interpretation of field-effect measurements, but also in studies involving point-contact spectroscopy, electromigration, and enhancement of conductivity by photoexcitation. The essential physics of the phenomenon is not new, as parallels exist with the Verwey transition in  $\text{Fe}_3\text{O}_4$ .

## ACKNOWLEDGMENTS

One of us (N.C.) gratefully acknowledges discussions with Dr. S. K. Kurtz, Dr. R. Baetzold, Dr. G. Shirane, Dr. J. Kirtley, Dr. A. Kleinsasser, and Dr. R. Sobolewski. This work was supported in part by the Materials Research Group program of the National Science Foundation under Grant No. NSF/DMR-8908094 and by the Air Force Office of Scientific Research under Grant No. F49620-93-1-0076.

- <sup>1</sup>R. E. Glover and M. D. Sherrill, *Phys. Rev. Lett.* **5**, 248 (1960).  
<sup>2</sup>A. T. Fiory, A. F. Hebard, R. H. Eick, P. M. Mankiewich, R. E. Howard, and M. L. O'Malley, *Phys. Rev. Lett.* **65**, 3441 (1990); J. Mannhart, D. G. Schlom, J. G. Bednorz, and K.A. Mueller, *ibid.* **67**, 2099 (1991).  
<sup>3</sup>X. X. Xi, Q. Li, C. Doughty, C. Kwon, S. Bhattacharya, A. T. Findikoglu, and T. Venkatesan, *Appl. Phys. Lett.* **59**, 3470 (1991); X. X. Xi, C. Doughty, A. Walkenhorst, C. Kwon, Q. Li, and T. Venkatesan, *Phys. Rev. Lett.* **68**, 1240 (1992).  
<sup>4</sup>A. W. Kleinsasser and W. J. Gallagher, in *Superconducting Devices*, edited by S. T. Ruggiero and D. A. Rudman (Academic, Boston, 1990), p. 325.  
<sup>5</sup>L. F. Rybal'chenko, V. V. Fisun, N. L. Bobrov, I. K. Yanson, A. V. Bondarenko, and M. A. Obolenskii, *Fiz. Nizk. Temp. (Kiev)* **17**, 202 (1991) [*Sov. J. Low Temp. Phys.* **17**, 105 (1991)].  
<sup>6</sup>B. W. Veal, H. You, A. P. Paulikas, H. Shi, Y. Fang, and J. W. Downey, *Phys. Rev. B* **42**, 4770 (1990).  
<sup>7</sup>G. Ceder, R. P. McCormack, and D. de Fontaine, *Phys. Rev. B* **44**, 2377 (1991).  
<sup>8</sup>B. H. Moeckley, D. K. Lathrop, and R. A. Buhrman, *Phys. Rev. B* **47**, 400 (1993).  
<sup>9</sup>S. J. Rothman, J. L. Routbort, and J. E. Barker, *Phys. Rev. B* **40**, 8852 (1989).  
<sup>10</sup>V. I. Kudinov, I. L. Chalygin, A. I. Kirilyuk, N. M. Kreines, R. Laiho, and E. Lahderanta, *Physica C* **185-189**, 751 (1991); V. I. Kudinov, A. I. Kirilyuk, N. M. Kreines, R. Laiho, and E. Lahderanta, *Phys. Lett. A* **157**, 290 (1991).  
<sup>11</sup>N. Chandrasekhar, Oriol T. Valls, and A. M. Goldman, *Phys. Rev. Lett.* **71**, 1079 (1993).  
<sup>12</sup>G. Nieva, E. Osquiquil, J. Guimpel, M. Maenhoudt, B. Wuyts, Y. Bruynseraede, M. B. Maple, and I. K. Schuller, *Appl. Phys. Lett.* **60**, 2159 (1992).  
<sup>13</sup>D. de Fontaine, L. T. Wille, and S. C. Moss, *Phys. Rev. B* **36**, 5709 (1987).  
<sup>14</sup>L. T. Wille and D. de Fontaine, *Phys. Rev. B* **37**, 2227 (1988).  
<sup>15</sup>J. Stolze, *Phys. Rev. Lett.* **64**, 970 (1990).  
<sup>16</sup>P. A. Sterne and L. T. Wille, *Physica C* **162**, 223 (1989).  
<sup>17</sup>V. Müller, C. Hucho, K. de Groot, and K. H. Rieder, *Physica B* **165&166**, 1271 (1990).  
<sup>18</sup>D. Mihailovic and I. Poberaj, *Physica C* **185-189**, 781 (1992).  
<sup>19</sup>S. K. Kurtz, A. Bhalla, and L. E. Cross, *Ferroelectrics* **117**, 261 (1991); S. K. Kurtz, L. E. Cross, N. Setter, D. Knight, A. Bhalla, W. W. Cao, and W. N. Lawless, *Mater. Lett.* **6**, 317 (1988).  
<sup>20</sup>A. Bussman-Holder, A. R. Bishop, A. Migliori, and Z. Fisk, *Ferroelectrics* **128**, 105 (1992).  
<sup>21</sup>V. Müller, C. Hucho, K. de Groot, D. Winau, D. Maurer, and K. H. Rieder, *Solid State Commun.* **72**, 997 (1989).  
<sup>22</sup>S. D. Conradson, I. D. Raistrick, and A. R. Bishop, *Science* **248**, 1394 (1990).  
<sup>23</sup>K. A. Müller, *Z. Phys. B* **80**, 193 (1990).  
<sup>24</sup>R. Baetzold, *Phys. Rev. B* **38**, 305 (1988).  
<sup>25</sup>R. Baetzold (private communication).  
<sup>26</sup>J. F. Nye, *Physical Properties of Crystals* (Clarendon, Oxford, 1990).  
<sup>27</sup>L. R. Testardi, W. G. Moulton, H. Mathias, H. K. Ng, and C. M. Rey, *Phys. Rev. B* **37**, 2324 (1988).  
<sup>28</sup>G. Ceder, M. Asta, and D. de Fontaine, *Physica C* **177**, 106 (1991).  
<sup>29</sup>J. Mannhart, *Mod. Phys. Lett. B* **6**, 555 (1992).  
<sup>30</sup>D. de Fontaine, M. Asta, G. Ceder, R. McCormack, and G. Van Tendeloo, *Europhys. Lett.* **19**, 229 (1993).  
<sup>31</sup>S. J. Rothman, J. L. Routbort, U. Welp, and J. E. Baker,

- Phys. Rev. B **44**, 2326 (1991).
- <sup>32</sup>S. M. Sze, *Physics of Semiconductor Devices* (Wiley, New York, 1981).
- <sup>33</sup>P. J. M. van Bentum, R. T. M. Smokers, and H. van Kempen, Phys. Rev. Lett. **60**, 2543 (1988).
- <sup>34</sup>R. Buhrman (private communication).
- <sup>35</sup>A. J. Melmed, P. P. Camus, N. Ernst, W. A. Schmidt, G. Bozdech, and M. Naschitzki, Surf. Sci. **246**, 173 (1991).
- <sup>36</sup>R. P. Feynman, Phys. Rev. **97**, 660 (1955).
- <sup>37</sup>R. P. Feynman, R. W. Hellwarth, C. K. Iddings, and P. M. Platzman, Phys. Rev. **127**, 1004 (1962).
- <sup>38</sup>K. K. Thornber and R. P. Feynman, Phys. Rev. B **1**, 4099 (1970).
- <sup>39</sup>J. R. Kirtley (private communication).
- <sup>40</sup>Li Liu, K. Zhang, H. M. Jaeger, D. B. Buchholz, and R. P. H. Chang (unpublished).
- <sup>41</sup>E. J. W. Verwey and P. W. Haayman, Physica **8**, 979 (1941); E. J. W. Verwey, P. W. Haayman, and F. C. Romeijn, J. Chem. Phys. **15**, 181 (1947).